J Fluoresc (2015) 25:707–717
DOI 10.1007/s10895-015-1556-7

ORIGINAL PAPER

Organization and Dynamics of Tryptophan Residues in Brain Spectrin: Novel Insight into Conformational Flexibility

Madhurima Mitra · Arunima Chaudhuri · Malay Patra · Chaitali Mukhopadhyay · Abhijit Chakrabarti · Amitabha Chattopadhyay

Received: 9 January 2015 / Accepted: 5 March 2015 / Published online: 3 April 2015

Abstract Brain spectrin enjoys overall structural and sequence similarity with erythroid spectrin, but less is known about its function. We utilized the fluorescence properties of tryptophan residues to monitor their organization and dynamics in brain spectrin. Keeping in mind the functional relevance of hydrophobic binding sites in brain spectrin, we monitored the organization and dynamics of brain spectrin bound to PRODAN. Results from red edge excitation shift (REES) indicate that the organization of tryptophans in brain spectrin is maintained to a considerable extent even after denaturation. These results are supported by acrylamide quenching experiments. To the best of our knowledge, these results constitute the first report of the presence of residual structure in urea-denatured brain spectrin. We further show from REES and time-resolved emission spectra that PRODAN bound to brain spectrin is characterized by motional restriction. These results provide useful information on the differences between erythroid spectrin and brain spectrin.

Keywords Brain spectrin · REES · Fluorescence quenching · PRODAN · Tryptophan · TRES

Madhurima Mitra and Arunima Chaudhuri contributed equally to this work.

M. Mitra
Biophysics and Structural Genomics Division, Saha Institute of Nuclear Physics, 1/AF Bidhannagar, Kolkata 700064, India

A. Chaudhuri · A. Chattopadhyay (✉)
CSIR-Centre for Cellular and Molecular Biology, Uppal Road, Hyderabad 500 007, India
e-mail: amit@ccmb.res.in

M. Patra · C. Mukhopadhyay
Department of Chemistry, University of Calcutta, 92, A.P.C. Road, Kolkata 700 009, India

A. Chakrabarti (✉)
Crystallography and Molecular Biology Division, Saha Institute of Nuclear Physics, 1/AF Bidhannagar, Kolkata 700 064, India
e-mail: abhijit.chakrabarti@saha.ac.in

Introduction

Spectrin is a major cytoskeletal protein lining the erythroid membrane and acts as a scaffold for other cytoplasmic protein association [1–3]. The elasticity of the membrane bilayer is modulated by the complex network composed of spectrin and other cytoskeletal proteins. In evolutionary terms, spectrin evolved with metazoan organisms to fulfill the requirement of structures that would strengthen cellular adhesion and stabilize the plasma membrane against the force of movement [4]. Interestingly, spectrin is responsible for maintenance of the phase-state asymmetry in erythrocyte membranes [5] and exhibits chaperone-like activity [6].

Spectrin is a heterodimer composed of two subunits α and β (with mol. wts. of 280 and 246 kDa, respectively). The two subunits share 30 % identity and are aligned in an antiparallel side-to-side orientation to form a flexible and highly elongated, worm-like, rod-shaped heterodimer with hydrophobic stretches, and the amino and carboxy termini are oriented toward the ends of the rods [3]. The primary sequence of spectrin is characterized by a series of contiguous motifs called 'spectrin repeats' (typically 106 amino acid repeating sequences) that are representative of all members of the spectrin family of proteins [7]. It has been proposed that these repeats could have been generated by gene duplication [8]. Dimeric spectrin has a number of tryptophan residues distributed over the entire molecule, with 42 tryptophans in each of the α and β subunits [9, 10]. The spectrin repeats are characterized by a strongly conserved tryptophan at the 45th position and partially conserved tryptophan at the 11th position. A

careful analysis reveals that there are 41 tryptophans in 23 repeat motifs in the α subunit and 35 tryptophans in 17 repeat motifs in the β subunit of the spectrin dimer. The importance of the repeat motifs with respect to tryptophans is apparent when one considers the fact that more than 90 % of the total tryptophans in the spectrin dimer are found in these positions (repeat motifs). In addition, some of the conserved tryptophans have been implicated in folding of the spectrin domains [11] and in maintaining thermodynamic stability [12, 13]. The interesting observation that tryptophans are distributed over the entire spectrin dimer and still are localized in conserved positions in each domain makes them convenient fluorescent reporters for exploring conformational changes in spectrin that contribute to its elastic deformability exhibited in physiological situations [12, 14, 15]. We have previously utilized the intrinsic tryptophan fluorescence of erythroid spectrin to monitor its conformational flexibility and interaction with micellar detergents [14–16]. A substantial number of spectrin tryptophans are close to hydrophobic patches that can bind hydrophobic ligands (such as fatty acids and phospholipids), thereby inducing quenching of tryptophan fluorescence [17, 18]. The hydrophobic stretches in spectrin provide binding surfaces to the hydrophobic, polarity sensitive fluorescent probe 6-propionyl-2-dimethylaminonaphthalene (PRODAN) [19]. We have previously shown that PRODAN binds to erythroid spectrin with a high affinity [20, 21].

Non-erythroid (brain) spectrin has a high degree of sequence homology with erythroid spectrin [22]. Brain spectrin, like erythroid spectrin, forms rod-shaped heterodimers in an antiparallel side-to-side orientation. Similar to erythroid spectrin, non-erythroid (brain) spectrin also contains conserved tryptophan residues at 43rd and 53rd positions in the α subunit and 17th position at the β subunit. In spite of the overall sequence and structural similarity between erythroid spectrin and brain spectrin, less is known about the function of brain spectrin. Brain spectrin in the axonal cytoskeleton has been implicated to be necessary for the stability of nascent sodium channel clusters [23]. Both erythroid spectrin and brain spectrin bind to membrane phospholipids [24]. However, the binding of anionic phospholipids is reported to be stronger (higher affinity) in case of brain spectrin [25]. Although the amino terminal region of the α subunit and carboxy terminal region of the β subunit of non-erythroid (brain) spectrin exhibit ~60 and 70 % similarity with corresponding regions of erythroid spectrin [26, 27], the two spectrin isoforms appear different in their structure and function. Crystal structure and phage-displayed single-chain variable fragment analysis show that the tetramerization site or the self-associating domain of brain spectrin is different from that of erythroid spectrin [28, 29]. This is further supported by the observation that the heterodimer of brain spectrin forms tetramer that is ~15 times stronger than the corresponding tetramer formed by erythroid spectrin [30]. Brain spectrin is more rigid and thermally stable than erythroid spectrin [31]. We have recently reported certain mechanistic differences in binding of the hydrophobic fluorescent probe PRODAN to erythroid spectrin and brain spectrin, as revealed by analysis of thermodynamic parameters [21].

In this work, we have explored the organization and dynamics of tryptophan residues in brain spectrin in native and urea-denatured conditions utilizing a variety of fluorescence approaches, keeping in mind their role in the structure and function of brain spectrin. In addition, in the overall context of the relevance of hydrophobic binding sites in brain spectrin, we monitored the organization and dynamics of PRODAN bound to brain spectrin using similar approaches. Our results show that the motional restriction experienced by tryptophans in brain spectrin is present to a considerable extent even in denatured state, implying that some of the structural and dynamic features of brain spectrin are retained under such condition. These observations therefore bring up the interesting possibility that brain spectrin preserves residual structures *even* after denaturation. These results assume relevance in the context of the role of tryptophans in the stability, folding and function of brain spectrin.

Experimental

Materials

Sepharose CL-4B column, Tris, KCl, phenylmethylsulfonyl fluoride (PMSF), dithiothreitol (DTT), EDTA, EGTA, imidazole, $MgCl_2$, NaCl, ammonium sulfate and ultrapure grade urea were obtained from Sigma Chemical Co. (St. Louis, MO). PRODAN was obtained from Molecular Probes/Invitrogen (Eugene, OR). Concentration of PRODAN in methanolic stock solution was calculated from its molar extinction coefficient (ε) of 18,000 M^{-1} cm^{-1} at 360 nm [19]. Ultrapure grade acrylamide was from Invitrogen/Life Technologies. The purity of acrylamide was checked from its absorbance using its molar extinction coefficient (ε) of 0.23 M^{-1} cm^{-1} at 295 nm and optical transparency beyond 310 nm [32]. All other chemicals used were of the highest purity available. Solvents used were of spectroscopic grade. Water was purified through a Millipore (Bedford, MA) Milli-Q system and used throughout.

Isolation and Purification of Brain Spectrin

Sheep brains of freshly sacrificed animals were obtained from a local slaughterhouse for purification of brain spectrin following the guidelines of the Institutional Animal and Bioethics Committee of Saha Institute of Nuclear Physics. Brain spectrin in its tetrameric form was purified from ovine brain as described earlier [21]. All the steps were carried out between 0 and 4 °C and all buffers contained PMSF. Fresh ovine brain was homogenized in 10 mM Tris buffer (pH 7.0) containing 1 mM EGTA, 5 mM

EDTA, 10 mM imidazole, 0.2 mM DTT and 0.2 mM PMSF and centrifuged for 1 h at 15,000×*g*. The pellet obtained was further homogenized in 10 mM Tris (pH 8.0) containing 5 mM $MgCl_2$, 1 mM EGTA, 0.6 mM EDTA, 0.2 mM DTT, and 0.2 mM PMSF. The salt concentration of the solution was adjusted to 0.6 M NaCl from stock NaCl solution and was stirred for 1 h at 4 °C; followed by centrifugation for 45 min at 15,000×*g*. The supernatant was passed through cheese cloth. Crude brain spectrin was obtained after further centrifugation at 12,000×*g* at 4 °C. Purified brain spectrin was obtained after concentrating with 50 % ammonium sulfate precipitation followed by Sepharose CL-4B column chromatography and stored in 1 mM sodium phosphate (pH 8.0) buffer containing 20 mM KCl, 0.2 mM DTT and 0.2 mM PMSF. The purity of the preparation was checked on 8 % SDS-PAGE under reducing condition. Before performing any fluorescence experiment, brain spectrin was dialyzed against 10 mM Tris buffer (pH 7.8) containing 20 mM KCl. Concentration of brain spectrin was determined by Bradford method with bovine serum albumin as a standard [33].

Sample Preparation and Steady State Fluorescence Measurements

Freshly prepared brain spectrin was maintained in 10 mM Tris buffer (pH 7.8) containing 20 mM KCl for all fluorescence measurements. Brain spectrin was denatured in 8 M urea by incubating in urea solution for 2 h prior to spectroscopic measurements. For studies on PRODAN bound to brain spectrin, PRODAN was incubated for 3 h with 2.5 times molar excess of brain spectrin. All experiments were carried out at room temperature (~23 °C).

Steady state fluorescence measurements were performed with a Hitachi F-7000 spectrofluorometer (Tokyo, Japan) using 1 cm path length quartz cuvette. Excitation and emission slits with a nominal bandpass of 3 nm were used for all measurements. All spectra were recorded using the correct spectrum mode. Background intensities of samples in which fluorophores were omitted were negligible in most cases and were subtracted from each sample spectrum to cancel out any contribution due to the solvent Raman peak and other scattering artifacts. The spectral shifts obtained with different sets of samples were identical in most cases, or were within ± 1 nm of the ones reported. Fluorescence anisotropy measurements were performed using a Hitachi polarization accessory. Anisotropy values were calculated from the equation [34]:

$$r = \frac{I_{VV} - GI_{VH}}{I_{VV} + 2GI_{VH}} \quad (1)$$

where I_{VV} and I_{VH} are the measured fluorescence intensities (after appropriate background subtraction) with the excitation polarizer vertically oriented and emission polarizer vertically and horizontally oriented, respectively. G is the grating correction factor and is the ratio of the efficiencies of the detection system for vertically and horizontally polarized light, and is equal to I_{HV}/I_{HH}. All experiments were performed with multiple sets of samples and average values of anisotropy are shown in the figures.

Fluorescence Quenching Measurements

Acrylamide quenching experiments of tryptophan fluorescence were carried out as described earlier [14] by measuring fluorescence intensity after serial addition of small aliquots of freshly prepared stock solution of 2 M acrylamide in water to a stirred sample followed by incubation for 3 min in the sample compartment in dark. The excitation wavelength used was 295 nm, and emission was monitored at 338 nm. The fluorescence intensities obtained were corrected for dilution. Corrections for inner filter effect were made using the following equation [34]:

$$F = F_{obs}\text{antilog}\left[(A_{ex} + A_{em})/2\right] \quad (2)$$

where F is the corrected fluorescence intensity and F_{obs} is the background subtracted fluorescence intensity of the sample (also corrected for dilution). A_{ex} and A_{em} are the measured absorbance at the excitation and emission wavelengths, respectively. Quenching data were analyzed by fitting to the Stern-Volmer equation [34]:

$$F_o/F = 1 + K_{SV}[Q] \quad (3)$$

where F_o and F are the fluorescence intensities in the absence and presence of the quencher (acrylamide), [Q] is the molar quencher concentration and K_{SV} is the Stern-Volmer quenching constant. In order to quantitate the fraction of fluorophores accessible to the quencher (f_a), the quenching data were also analyzed using a modified equation by Lehrer [35]:

$$F_o/\Delta F = 1/(K_a f_a[Q]) + 1/f_a \quad (4)$$

where $\Delta F = F_o - F$, K_a is the Stern-Volmer quenching constant for the accessible fraction and f_a is the fraction of initial fluorescence accessible to the quencher.

Time-Resolved Emission Spectra (TRES) Measurements

Fluorescence lifetimes were calculated from time-resolved fluorescence intensity decays using IBH 5000 F NanoLED equipment (Horiba Jobin Yvon, Edison, NJ) with Data Station software in the time-correlated single photon counting mode as described earlier [36]. A pulsed light-emitting diode (LED) (NanoLED-16) was used as an excitation source. This LED generates optical pulse at 337 nm of pulse duration 1.2 ns and is run at 1 MHz repetition rate. LED profile (instrument

response function) was measured at the excitation wavelength using Ludox (colloidal silica) as the scatterer. To optimize the signal-to-noise ratio, 10,000 photon counts were collected in the peak channel. All experiments were performed using emission slits with a bandpass of 4 nm or less. The sample and the scatterer were alternated after every 5 % acquisition to ensure compensation for any shape and timing drifts that could occur during the period of data collection. This arrangement also prevents any prolonged exposure of the sample to the excitation beam, thereby avoiding any possible photodamage to the fluorophore. Data were stored and analyzed using DAS 6.2 software (Horiba JobinYvon, Edison, NJ). Fluorescence intensity decay curves so obtained were deconvoluted with the instrument response function and analyzed as a sum of exponential terms:

$$F(t) = \Sigma_i \alpha_i \exp(-t/\tau_i) \quad (5)$$

where F(t) is fluorescence intensity at time t and α_i is a pre-exponential factor representing the fractional contribution to the time-resolved decay of the component with a lifetime τ_i such that $\Sigma_i \alpha_i = 1$. Decay parameters were recovered using a nonlinear least squares iterative fitting procedure based on the Marquardt algorithm. TRES was generated as described earlier [36]. For this, a series of fluorescence decays were acquired over a range of emission wavelengths (400–500 nm) across the emission spectrum, using a constant excitation wavelength of 337 nm. All the decay curves were then individually fitted as a sum of exponential terms as discussed above. The net result of such an analysis was a set of deconvoluted intensity decays at various emission wavelengths, i.e., a three-dimensional data set of counts vs. time vs. emission wavelength. This three-dimensional data set was sliced orthogonally to the time axis to produce two-dimensional spectra of counts vs. emission wavelength in order to visualize how the emission spectrum evolves during the fluorescence lifetime. This approach has the advantage that convolution distortion is avoided because each decay curve is individually deconvoluted before the construction of the final TRES plot.

Circular Dichroism (CD) Measurements

Far-UV CD measurements were carried out at room temperature (~23 °C) on a BioLogic Science Instruments (France) MOS-450 spectropolarimeter. Spectra were measured in a quartz optical cell with a pathlength of 0.1 mm and recorded in 1 nm wavelength increments and band width of 5 nm. The scan rate was 0.5 nm/s and each spectrum was the average of 5 scans. All spectra were corrected for background by subtraction of appropriate blanks without brain spectrin. The spectra were subjected to a moderate degree of noise-reduction analysis by smoothing making sure that the overall shape of the spectrum remains unaltered. Data are represented as mean residue ellipticities and calculated using the equation:

$$[\theta] = \theta_{obs}/(10Cl) \quad (6)$$

where θ_{obs} is the observed ellipticity in mdeg, l is the path length in cm, and C is the concentration of peptide bonds in mol/L.

Results

Fluorescence and Circular Dichroism Signatures of Urea-Denatured Brain Spectrin

Figure 1 shows the fluorescence emission spectra of brain spectrin in native and urea denatured states. As shown in the figure, tryptophans in native brain spectrin exhibit an emission maximum at 338 nm, similar to emission maximum of erythroid spectrin [14]. The figure also shows that the fluorescence emission spectrum of brain spectrin denatured with urea displays a red shifted emission maximum and is at 350 nm. This red shift can be attributed to increased exposure of tryptophans in brain spectrin to water upon urea denaturation. Interestingly, tryptophan in water (i.e., fully exposed) exhibits an emission maximum at 355 nm [37]. The emission maximum of 350 nm for denatured brain spectrin therefore indicates that the tryptophans are shielded from bulk water to a certain extent (see later), even when denatured in 8 M urea.

The corresponding CD spectra of native and denatured brain spectrin are shown in Fig. 2. The backbone CD spectrum of native brain spectrin is characteristic of a protein with predominantly α-helical structure, in agreement with earlier

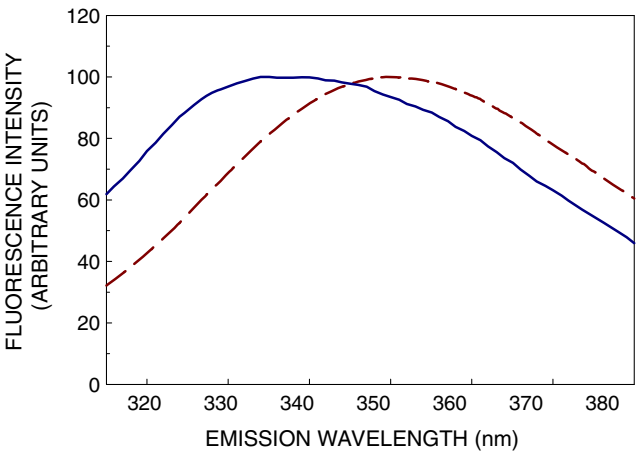

Fig. 1 Tryptophan fluorescence emission spectra of brain spectrin in native and urea-denatured conditions. Representative fluorescence emission spectra of brain spectrin in native (—) and urea denatured (– – –) states. The concentration of native and urea denatured brain spectrin were 0.6 and 0.4 μM, respectively. The excitation wavelength was 295 nm. Brain spectrin was denatured in 8 M urea. The fluorescence spectra are intensity normalized at the emission maximum. See Experimental for other details

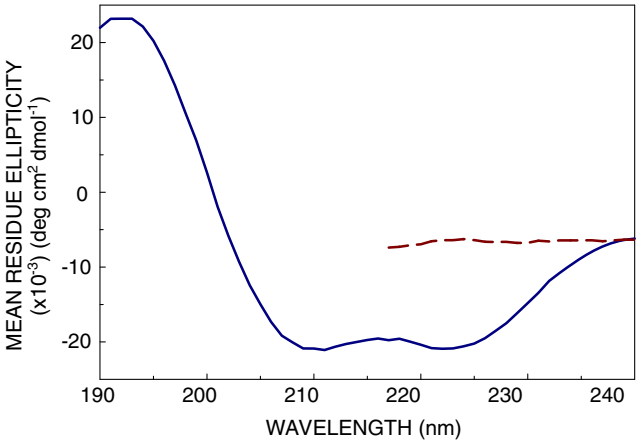

Fig. 2 Secondary structure of brain spectrin in native and urea-denatured conditions. Far-UV CD spectra of brain spectrin in native (—) and urea denatured (- - -) states. The concentration of brain spectrin was 0.2 μM. CD data below 215 nm were not recorded for urea-denatured brain spectrin due to high absorbance of urea in this wavelength range. All other conditions are as in Fig. 1. See Experimental for other details

report [38]. When denatured in urea, the CD spectrum of brain spectrin displayed considerable loss of helicity, indicating loss of secondary structure elements.

Red Edge Excitation Shift of Brain Spectrin in Native and Urea-Denatured States

Red edge excitation shift (REES) is operationally defined as the shift in the wavelength of maximum fluorescence emission toward higher wavelengths, caused by a shift in the excitation wavelength toward the red edge of the absorption band. The dipolar relaxation time of the solvent shell around a polar fluorophore becomes comparable to or longer than its fluorescence lifetime in motionally restricted environment and this gives rise to photoselection of differentially relaxed population of fluorophores upon excitation toward the red edge [39–44]. The fact that the fluorophore in REES measurements merely acts as a reporter group and allows to monitor the mobility parameters of the environment itself (represented by the relaxing solvent molecules) adds to its uniqueness. This attractive aspect of REES has proved to be a convenient tool to monitor organization and dynamics of probes and proteins in membranes and membrane-mimetic environments [45–52], and tryptophans in soluble proteins [53–56].

The shifts in the maxima of fluorescence emission[1] of brain spectrin as a function of excitation wavelength are shown in

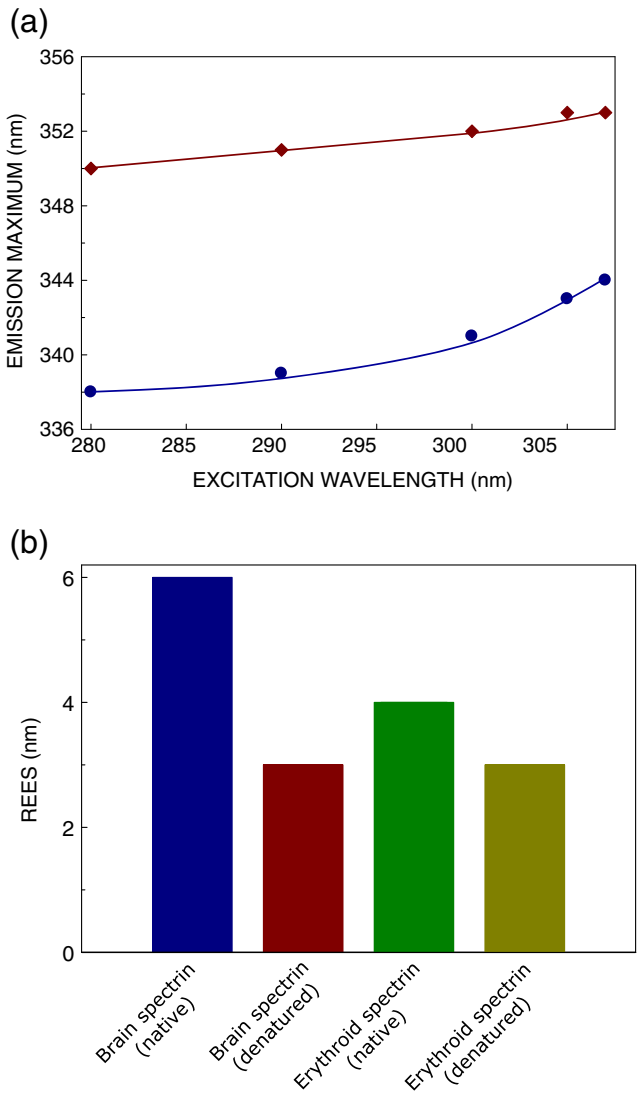

Fig. 3 REES exhibited by brain spectrin in native and urea-denatured conditions. **a** Effect of changing excitation wavelength on the wavelength of maximum emission for native (●) and urea-denatured (♦) brain spectrin. *Lines* joining the data points are provided merely as viewing guides. **b** The magnitude of REES, which corresponds to the shift in emission maximum when the excitation wavelength was changed from 280 to 307 nm, exhibited by native and denatured states of brain spectrin are shown. REES of native and denatured states of erythroid spectrin under comparable conditions (taken from ref. [14]) are also shown for comparison. All other conditions are as in Fig. 1. See Experimental for other details

Fig. 3a. Upon excitation at 280 nm, tryptophans in native brain spectrin exhibited an emission maximum at 338 nm (see above; Fig. 1). As the excitation wavelength is changed from 280 to 307 nm, the emission maximum of native brain spectrin is shifted from 338 to 344 nm, which corresponds to a REES of 6 nm (see Fig. 3b). It was practically difficult to monitor any further red shift when native brain spectrin was excited beyond 307 nm due to very low signal to noise ratio, and artifacts due to the solvent Raman peak that sometimes remained even after background subtraction. Such type of

[1] We have used the term maximum of fluorescence emission in a somewhat broader sense here. In every case, we have monitored the wavelength corresponding to maximum fluorescence intensity, as well as the center of mass of the fluorescence emission, in the symmetric part of the spectrum. In most cases, both these methods yielded the same wavelength. In cases where minor discrepancies were found, the center of mass of emission has been reported as the fluorescence maximum.

shift in the wavelength of emission maximum with corresponding change in excitation wavelength is representative of REES and indicates that the tryptophans in native brain spectrin experience motionally restricted environment. Since brain spectrin is a multi-tryptophan protein, REES in this case is indicative of the average environment experienced by the tryptophans. Nonetheless, such a result would imply that the regions surrounding a sub-population of tryptophans in brain spectrin offer considerable restriction to the reorientational motion of the solvent (water) dipoles in the excited state. Interestingly, it has been previously reported that some of the tryptophans in brain spectrin are shielded from the bulk solvent [11, 13]. This population of tryptophans is more likely to contribute to the observed REES of brain spectrin. In addition, many of these tryptophans are at or in the vicinity of hydrophobic patches in brain spectrin [57] which can bind hydrophobic ligands and the estimated apparent dielectric constant of the hydrophobic binding site(s) are low [21]. The low dielectric environment of these hydrophobic patches are generally characterized by restricted solvent molecules, rendering these regions suitable for displaying REES and other wavelength-selective effects [40,43,44; see later]. Interestingly, the magnitude of REES exhibited by tryptophans in native brain spectrin is higher compared to tryptophans in erythroid spectrin (see Fig. 3b). This is indicative of possible difference in the microenvironment around the tryptophans in erythroid spectrin compared to brain spectrin.

Interestingly, REES effects are still observed in case of denatured brain spectrin. As the excitation wavelength is changed from 280 to 307 nm, the emission maximum of the tryptophans in denatured brain spectrin displays a shift from 350 to 353 nm, which corresponds to a REES of 3 nm (see Fig. 3b). Exposure of the tryptophans in denatured state to bulk solvent leads to fast solvent relaxation, and therefore tryptophans in denatured proteins generally do not exhibit REES [53, 58]. However, we have previously reported that in rare cases (such as erythroid spectrin [14] and α-lactalbumin [55]) tryptophans in denatured proteins could show REES, thereby implying the presence of residual structures in these proteins that remain even after denaturation. This result, along with the emission maximum of 350 nm for denatured brain spectrin, indicates that the tryptophan microenvironment in brain spectrin maintains some of its organization (residual structure) even after denaturation. To the best of our knowledge, these results constitute the first report of the presence of such residual structure in denatured brain spectrin. These results gain further support from analysis of quenching of tryptophan fluorescence in brain spectrin by the water soluble quencher acrylamide (discussed below).

In addition to the shift in emission maximum upon red edge excitation, fluorescence anisotropy is known to be dependent on excitation wavelength in motionally restricted media [39]. The solvent relaxed state of the fluorophore (photoselected progressively toward the red edge of excitation) exhibits a decreased rotational rate, thereby increasing anisotropy, i.e., an increase in anisotropy is generally observed with increase in excitation wavelength. This is attributed to the strong dipolar interactions with the surrounding solvent molecules. This is illustrated in Fig. 4. The figure shows that the anisotropy of tryptophans in brain spectrin in the native state exhibited an increase of ~42 % upon altering the excitation wavelength from 295 to 305 nm. The corresponding increase in anisotropy for denatured brain spectrin when the excitation wavelength was increased from 295 to 305 nm was less (~22 %). Such characteristic increase in anisotropy upon red edge excitation for peptides and proteins containing tryptophans, especially in restricted environments has been previously reported [14, 53, 55]. Another possible reason for the increase in anisotropy at the red edge of excitation could be the reduced efficiency of self energy transfer (homo-FRET) among tryptophan residues, sometimes referred to as Weber's red edge effect [59, 60].

Acrylamide Quenching of Tryptophan Fluorescence: Evidence of Residual Structure in Urea-Denatured State

Acrylamide quenching of tryptophan fluorescence represents an extensively used approach to monitor the solvent accessibility of tryptophans in proteins [61]. A representative Stern-Volmer plot of acrylamide quenching of tryptophans in brain spectrin in native and denatured state is shown in Fig. 5a. The accessibility, i.e., the degree of solvent exposure of tryptophans in brain spectrin, is gleaned from the slope (K_{SV}) of the plot. The quenching parameters obtained by analyzing the Stern-Volmer plot are shown in Table 1. The Stern-

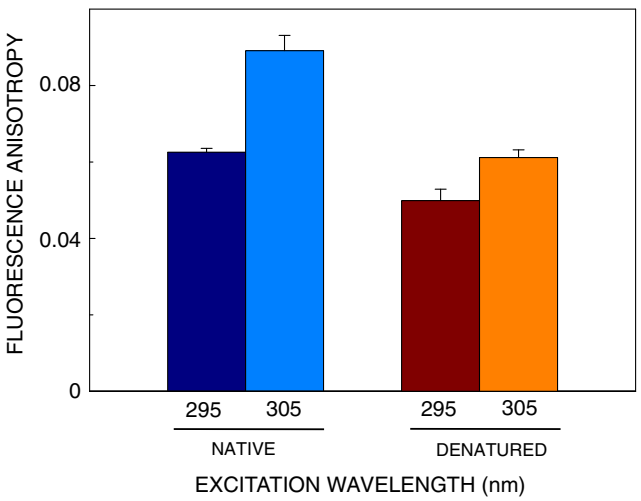

Fig. 4 Motional restriction experienced by tryptophans in brain spectrin in native and urea-denatured states. Fluorescence anisotropy of native and urea denatured brain spectrin is shown. The excitation wavelengths were 295 and 305 nm. Emission was monitored at 337 nm. All other conditions are as in Fig. 1. See Experimental for other details

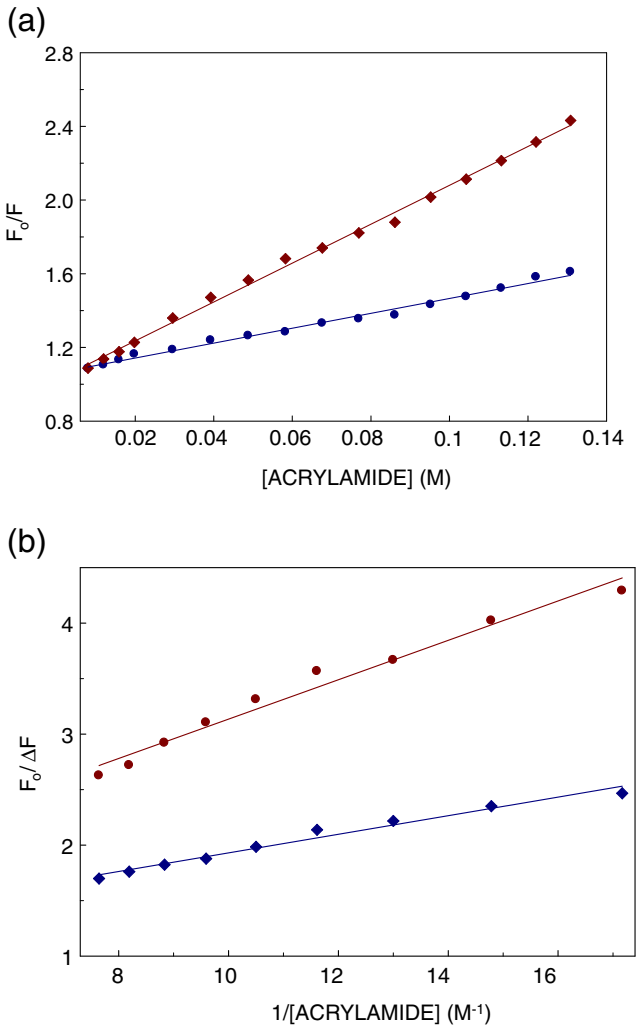

Fig. 5 Solvent exposure of tryptophans in brain spectrin in native and denatured conditions. Representative data for (**a**) Stern-Volmer and (**b**) Lehrer analysis of acrylamide quenching of native (●) and denatured (♦) states of brain spectrin. F_o is the tryptophan fluorescence in the absence of quencher (acrylamide), F is the corrected tryptophan fluorescence in the presence of quencher, and $\Delta F = F_o - F$. The concentration of brain spectrin was 0.2 μM. The excitation wavelength was 295 nm, and emission was monitored at 338 nm in all cases. See Experimental for other details

Volmer constant (K_{SV}) for acrylamide quenching of native brain spectrin was 4.41 M^{-1}. The value of K_{SV} was found to increase for urea denatured brain spectrin to 10.59 M^{-1}, indicating increased exposure of tryptophans upon denaturation. However, this value of K_{SV} is significantly low in comparison to the value of K_{SV} (13.42 M^{-1}) for fully exposed tryptophans as in the case of the model compound N-acetyl-L-tryptophanamide (NATA) in 8 M urea (see Table 1; [14]). This result indicates that even when denatured with 8 M urea, tryptophans in brain spectrin are not fully exposed and are shielded from the bulk aqueous environment, in agreement with our REES results (see Fig. 3). These results are further supported by Lehrer analysis [35] of the quenching data

Table 1 Acrylamide quenching of tryptophan fluorescence of brain spectrin[a]

Condition	K_{SV}[b] (M^{-1})	f_a[c]
Native	4.41±0.04	0.65±0.02
Denatured	10.59±0.01	0.87±0.03
NATA (8 M)	13.42±0.30[d]	

[a] Concentration of brain spectrin was 0.2 μM

[b] Calculated using Eq. (3). The quenching parameter shown represents means ± SE of at least three independent measurements while quenching data shown in Fig. 5a are from representative experiments

[c] Calculated using Eq. (4). The quenching parameter shown represents means ± SE of at least three independent measurements while quenching data shown in Fig. 5b are from representative experiments

[d] From ref. [14]

(shown in Fig. 5b). The higher accessibility of tryptophans in the denatured state of brain spectrin is further supported by Lehrer analysis, which shows that ~87 % of the tryptophan fluorescence was accessible in this state (see Table 1). Although these results indicate that tryptophans in brain spectrin are still not accessible even when denatured, the extent of tryptophan inaccessibility is higher in erythroid spectrin [14]. This could be due to differential stability and folding of brain spectrin and erythroid spectrin.

REES and TRES of PRODAN Bound to Brain Spectrin

Some of the tryptophan residues in brain spectrin are localized at or in the vicinity of hydrophobic patches which can bind ligands such as pyrene, fatty acids and phospholipids and cause quenching of tryptophan fluorescence [21, 57]. The hydrophobic patches are useful in the interaction of brain spectrin with membranes. In order to explore the microenvironment of these functionally important hydrophobic sites characterized by low polarity [21], we carried out REES measurements utilizing the fluorescence of the hydrophobic, polarity-sensitive probe PRODAN (see inset in Fig. 6a) bound to brain spectrin. We have previously shown that PRODAN binds to brain spectrin with a high affinity (apparent K_d~0.16 μM) [21].

A large change in the dipole moment of the fluorophore upon excitation, which causes the solvent dipoles to reorient in an energetically favorable manner in response to the altered dipole moment in the excited state, is an important requirement for a fluorophore to be able to exhibit REES [43]. PRODAN fluorescence is very sensitive to the polarity of the environment and its dipole moment changes by ~5–8 D upon excitation [62, 63]. A change in dipole moment of this magnitude, coupled with its hydrogen bonding capability [63] makes PRODAN an ideal probe for REES measurements. The shifts in the maxima of fluorescence emission of PRODAN bound to brain spectrin as a function of excitation wavelength are shown in Fig. 6. PRODAN shows an emission maximum

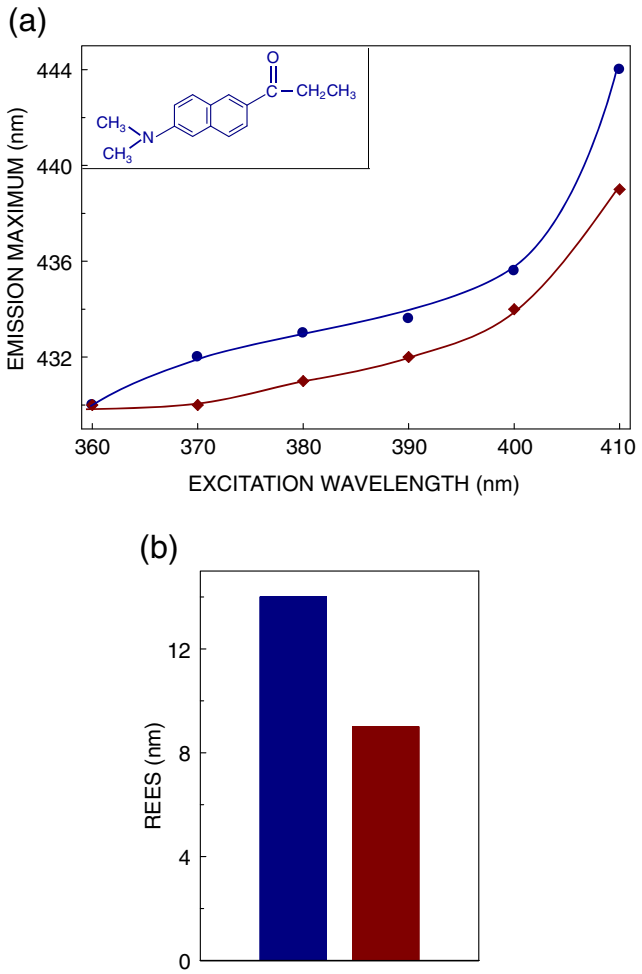

Fig. 6 REES of PRODAN bound to brain spectrin. **a** Effect of changing excitation wavelength on the wavelength of maximum emission for PRODAN bound to brain spectrin (●). Similar data for PRODAN bound to erythroid spectrin under comparable conditions (♦; taken from ref. [14]) are also shown for comparison. Lines joining data points are provided merely as viewing guides. The concentration of PRODAN was 0.2 μM, and that of brain spectrin was 0.5 μM. The chemical structure of PRODAN is shown in the *inset*. **b** The magnitude of REES, which corresponds to the shift in emission maximum when the excitation wavelength was changed from 360 to 410 nm, for PRODAN bound to brain spectrin is shown (*left bar*). REES of PRODAN bound to erythroid spectrin under comparable conditions (*right bar*, taken from ref. [14]) are also shown for comparison. See Experimental for other details

of 520 nm in water [20] which exhibits a blue shift of 90 nm when bound to brain spectrin indicating the nonpolar nature of the binding site. Figure 6 shows that when excited at 360 nm, PRODAN bound to brain spectrin exhibits a blue shifted emission maximum at 430 nm. As the excitation wavelength is changed from 360 to 410 nm, the emission maxima of PRODAN bound to brain spectrin is shifted from 430 to 444 nm, which amounts to a relatively large REES of 14 nm. This indicates that PRODAN bound to brain spectrin is in a motionally restricted environment. This would imply that the PRODAN-binding site in brain spectrin offers considerable restriction to the reorientational motion of the solvent dipoles around the excited state fluorophore. Figure 6b shows that the magnitude of REES experienced by PRODAN bound to brain spectrin is larger than when bound to erythroid spectrin. This is indicative of the difference in nature of the hydrophobic binding site in erythroid spectrin and brain spectrin. This is in overall agreement with the difference in binding affinity of PRODAN with brain spectrin and erythroid spectrin (binding is tighter with brain spectrin) [21].

Figure 7 shows the time-resolved emission spectra (TRES) of PRODAN bound to brain spectrin at early (up to 22.4 ns after excitation), and late (up to 33.6 ns after excitation time points.) A red shift in the emission spectrum of PRODAN with time is evident from the figure. For the early time point spectrum, the emission maximum is at ~430 nm, which shifts to ~460 nm for the late time point. In addition to static REES (Fig. 6), our results show that PRODAN bound to brain spectrin exhibits a dynamic change in emission maximum ('dynamic REES'), i.e., there is a change in the emission spectra of bound PRODAN during the fluorescence lifetime, indicative of relatively slow solvent relaxation in the excited state.

Discussion

In this work, we have explored the environment of tryptophan residues in brain spectrin in native and urea-denatured states utilizing a battery of fluorescence approaches. Since tryptophan residues are localized in chosen positions in brain spectrin sequence in the 106 long amino acid repeat units, and are conserved to a large extent, they are believed to be

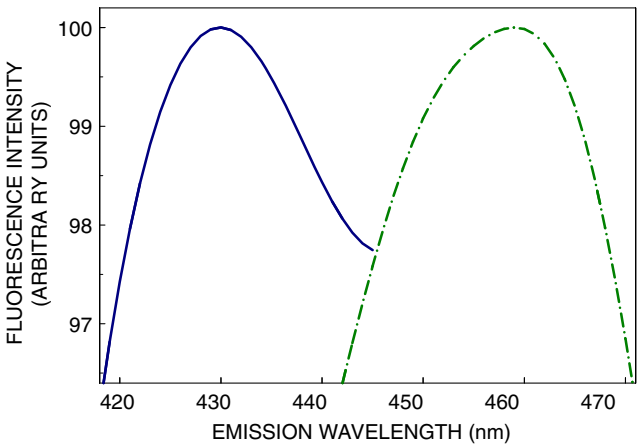

Fig. 7 TRES of PRODAN bound to brain spectrin reconstructed from fluorescence decays measured at different emission wavelengths across the emission spectrum. The emission spectra correspond to early ((—), up to 22.4 ns after excitation), and late ((- - -), up to 33.6 ns after excitation) time points. Spectra acquired at early and late time points correspond to initial (unrelaxed) excited state and fully relaxed excited state. The emission maximum gradually moves toward the red edge of the spectrum with time. Both spectra are intensity-normalized at the emission maximum. Excitation wavelength used was 337 nm. See Experimental for other details

important for the function of the protein. We report REES of 6 nm for tryptophans in brain spectrin in the native state. The exhibition of REES by tryptophans in native state brain spectrin is indicative of an ordered environment and reflects that the regions surrounding at least some of the tryptophans in brain spectrin offer considerable restriction to the reorientational motion of the solvent (water) dipoles around the excited state tryptophans. This is in agreement with previous reports describing a population of tryptophans in brain spectrin not being accessible to bulk solvent [11, 13]. This is further supported by tryptophan accessibility observed using acrylamide quenching. Interestingly, brain spectrin exhibits REES of 3 nm even after denaturation, similar to denatured erythroid spectrin [14]. This is clearly indicative of the distinct structural and dynamic features of brain spectrin that are maintained to a considerable extent even after denaturation. These results are reinforced by acrylamide quenching experiments in which the accessibility of the tryptophans in brain spectrin was assessed in native and denatured conditions.

It is generally believed that tryptophan residues in denatured proteins do not exhibit REES since they are exposed to bulk water characterized with fast relaxation [53, 58]. Our present results show that brain spectrin belongs to the short but growing list of proteins which show REES even when denatured [14, 55]. An interesting common feature of these proteins (which display REES even when denatured) is that all these proteins are characterized with hydrophobic stretches and membrane binding. The relevance of these observations may become clearer as we generate more data on this class of proteins. Interestingly, it has been previously reported that tryptophan residues can stabilize native-like structures in a denatured protein [64].

In addition, we have monitored the organization and dynamics of PRODAN bound to brain spectrin. When bound to brain spectrin, PRODAN exhibits REES of 14 nm indicating that PRODAN is in an environment where its mobility is considerably reduced. The motionally restricted environment of PRODAN bound to brain spectrin is further supported by time-resolved emission spectra characterized by dynamic Stokes shift, which indicates relatively slow solvent relaxation in the excited state. As mentioned earlier, PRODAN tends to bind to hydrophobic patches in proteins due to its hydrophobicity, and such binding in case of brain spectrin offers considerable restriction to the reorientational motion of the solvent dipoles around the excited state fluorophore. These hydrophobic sites could play a pivotal role in membrane binding function of brain spectrin [24, 25].

Our results merit comment in the context of the paucity in literature on the comparison of the biophysical properties of erythroid and brain spectrin. A much larger body of literature exists on erythroid spectrin compared to brain spectrin. Our REES results show that the tryptophans are probably located in a more ordered microenvironment in native brain spectrin compared to erythroid spectrin. Previous thermal studies have shown that the melting temperature for intact brain spectrin is higher than that of erythroid spectrin [31, 65], implying tissue-specific functional adaptability. Erythroid spectrin confers more elasticity required for red blood cells compared to brain spectrin which lines the postsynaptic contacts [66, 67] and appears stiffer and straighter, as monitored by electron microscopy [65]. This is supported by REES results of PRODAN bound to brain spectrin showed that the microenvironment around these regions offer more restriction to solvent relaxation (Fig. 6).

The two forms of spectrin also show differences in their urea-denatured forms. The accessibility of tryptophans to acrylamide quenching is higher for brain spectrin compared to the erythroid form in the urea-denatured state (see Table 1 and ref. [14]). We recently reported an extensive study monitoring the effects of denaturants, urea and guanidine hydrochloride, on the two forms of spectrin [68]. These results show that denaturation reaches a saturation in the presence of ~6–7 M urea. Although urea can be dissolved in pure water up to ~10 M, we chose not to carry out experiments beyond 8 M, since the saturating concentration drops after addition of protein, which leads to crystallization of urea. We also avoided performing thermal unfolding measurements since a major disadvantage of the method is that many proteins aggregate at high temperatures.

There has been a growing realization that denatured proteins often have a significant amount of residual structure which plays a crucial role in folding and stability of proteins [69–74]. Denatured states of proteins are of interest in protein folding studies not only in the context of the energetics of protein folding, but also for their potential contribution to the understanding of the functional aspects of proteins. The denatured state of a protein, which is a close in vitro approximation to the nascent polypeptide chains synthesized on the ribosomes, is the form recognized by chaperones. Such states are also recognized by a variety of protease systems responsible for intracellular protein turnover and by protein complexes that initiate transport across biological membranes.

In summary, our results provide novel information into the organization and dynamics of tryptophans and hydrophobic sites in brain spectrin which could be important in protein-protein interaction, signal transduction and interaction of brain spectrin with membranes. In addition, our results bring out subtle, yet what could turn out to be relevant differences between erythroid spectrin and brain spectrin. We envision that these results would be potentially useful in future efforts to decipher brain spectrin function.

Acknowledgments This work was supported by the Department of Atomic Energy (IBOP project) and the Council of Scientific and Industrial Research, Govt. of India. Ar.C. thanks the Council of Scientific and Industrial Research for the award of a Senior Research Fellowship. M.P. acknowledges the award of a Senior Research Fellowship from the University Grants Commission (India). A.C. gratefully acknowledges

support from J.C. Bose Fellowship (Department of Science and Technology, Govt. of India). A.C. is an Adjunct Professor of Jawaharlal Nehru University (New Delhi), Indian Institute of Science Education and Research (Mohali), Indian Institute of Technology (Kanpur) and Honorary Professor of the Jawaharlal Nehru Centre for Advanced Scientific Research (Bangalore). We thank Sourav Haldar for help with the TRES measurements, G. Aditya Kumar for help in making figures, and members of the Chattopadhyay laboratory for their comments and discussions.

Compliance with Ethical Standards

Conflict of Interest The authors declare that there is no conflict of interest.

Research Involving Human Participants and/or Animals Sheep brains of freshly sacrificed animals were obtained from a local slaughterhouse for purification of brain spectrin following the guidelines of the Institutional Animal and Bioethics Committee of Saha Institute of Nuclear Physics.

References

1. Bennett V, Gilligan DM (1993) The spectrin-based membrane skeleton and micron-scale organization of the plasma membrane. Annu Rev Cell Biol 9:27–66
2. Winkelmann JC, Forget BG (1993) Eythroid and nonerythroid spectrins. Blood 81:3173–3185
3. Chakrabarti A, Kelkar DA, Chattopadhyay A (2006) Spectrin organization and dynamics: new insights. Biosci Rep 26:369–386
4. Bennett V, Baines AJ (2001) Spectrin and ankyrin-based pathways: metazoan inventions for integrating cells into tissues. Physiol Rev 81: 1353–1392
5. Williamson P, Bateman J, Kozarsky K, Mattocks K, Hermanowicz N, Choe H-R, Schlegel RA (1982) Involvement of spectrin in the maintenance of phase-state asymmetry in the erythrocyte membrane. Cell 30:725–733
6. Bhattacharyya M, Ray S, Bhattacharya S, Chakrabarti A (2004) Chaperone activity and prodan binding at the self-associating domain of erythroid spectrin. J Biol Chem 279:55080–55088
7. Pascual J, Pfuhl M, Walther D, Saraste M, Nilges M (1997) Solution structure of the spectrin repeat: a left-handed antiparallel triple-helical coiled-coil. J Mol Biol 273:740–751
8. Viel A (1999) α-Actinin and spectrin structures: an unfolding family story. FEBS Lett 460:391–394
9. Sahr KE, Laurila P, Kotula L et al (1990) The complete cDNA and polypeptide sequences of human erythroid α-spectrin. J Biol Chem 265:4434–4443
10. Winkelmann JC, Chang J-G, Tse WT, Scarpa AL, Marchesi VT, Forget BG (1990) Full-length sequence of the cDNA for human erythroid β-spectrin. J Biol Chem 265:11827–11832
11. MacDonald RI, Musacchio A, Holmgren RA, Saraste M (1994) Invariant tryptophan at a shielded site promotes folding of the conformational unit of spectrin. Proc Natl Acad Sci U S A 91:1299–1303
12. Subbarao NK, MacDonald RC (1994) Fluorescence studies of spectrin and its subunits. Cell Motil Cytoskeleton 29:72–81
13. Pantazatos DP, MacDonald RI (1997) Site-directed mutagenesis of either the highly conserved Trp-22 or the moderately conserved Trp-95 to a large, hydrophobic residue reduces the thermodynamic stability of a spectrin repeating unit. J Biol Chem 272:21052–21059
14. Chattopadhyay A, Rawat SS, Kelkar DA, Ray S, Chakrabarti A (2003) Organization and dynamics of tryptophan residues in erythroid spectrin: novel structural features of denatured spectrin revealed by the wavelength-selective fluorescence approach. Protein Sci 12:2389–2403
15. Kelkar DA, Chattopadhyay A, Chakrabarti A, Bhattacharyya M (2005) Effect of ionic strength on the organization and dynamics of tryptophan residues in erythroid spectrin: a fluorescence approach. Biopolymers 77:325–334
16. Ray S, Chakrabarti A (2003) Erythroid spectrin in miceller detergents. Cell Motil Cytoskeleton 54:16–28
17. Sikorski AF, Michalak K, Bobrowska M (1987) Interaction of spectrin with phospholipids. Quenching of spectrin intrinsic fluorescence by phospholipid suspensions. Biochim Biophys Acta 904:55–60
18. Kahana E, Pinder JC, Smith KS, Gratzer WB (1992) Fluorescence quenching of spectrin and other red cell membrane cytoskeletal proteins. Relation to hydrophobic binding sites. Biochem J 282:75–80
19. Weber G, Farris FJ (1979) Synthesis and spectral properties of a hydrophobic fluorescent probe: 6-propionyl-2-(dimethylamino)naphthalene. Biochemistry 18:3075–3078
20. Chakrabarti A (1996) Fluorescence of spectrin-bound prodan. Biochem Biophys Res Commun 226:495–497
21. Patra M, Mitra M, Chakrabarti A, Mukhopadhyay C (2014) Binding of polarity- sensitive hydrophobic ligands to erythroid and nonerythroid spectrin: fluorescence and molecular modeling studies. J Biomol Struct Dyn 32:852–865
22. Leto TL, Fortugno-Erikson D, Barton D et al (1988) Comparison of nonerythroid α-spectrin genes reveals strict homology among diverse species. Mol Cell Biol 8:1–9
23. Voas MG, Lyons DA, Naylor SG, Arana N, Rasband MN, Talbot WS (2007) αII-Spectrin is essential for assembly of the nodes of Ranvier in myelinated axons. Curr Biol 17:562–568
24. Diakowski W, Sikorski AF (1995) Interaction of brain spectrin (fodrin) with phospholipids. Biochemistry 34:13252–13258
25. Diakowski W, Sikorski AF (2002) Brain spectrin exerts much stronger effect on anionic phospholipid monolayers than erythroid spectrin. Biochim Biophys Acta 1564:403–411
26. Li Q, Fung LW-M (2009) Structural and dynamic study of the tetramerization region of non-erythroid α-spectrin: a frayed helix revealed by site-directed spin labeling EPR. Biochemistry 48:206–215
27. Mehboob S, Jacob J, May M, Kotula L, Thiyagarajan P, Johnson ME, Fung LW-M (2003) Structural analysis of the αN-terminal region of erythroid and nonerythroid spectrin by small-angle X-ray scattering. Biochemistry 42:14702–14710
28. Mehboob S, Song Y, Witek M, Long F, Santarsiero BD, Johnson ME, Fung LW-M (2010) Crystal structure of the nonerythroid α-spectrin tetramerization site reveals differences between erythroid and nonerythroid spectrin tetramer formation. J Biol Chem 285:14572–14584
29. Song Y, Antoniou C, Memic A, Kay BK, Fung LW-M (2011) Apparent structural differences at the tetramerization region of erythroid and nonerythroid beta spectrin as discriminated by phage displayed scFvs. Protein Sci 20:867–879
30. Begg GE, Morris MB, Ralston GB (1997) Comparison of the salt-dependent self-association of brain and erythroid spectrin. Biochemistry 36:6977–6985
31. An X, Zhang X, Salomao M, Guo X, Yang Y, Wu Y, Gratzer W, Baines AJ, Mohandas N (2006) Thermal stabilities of brain spectrin and the constituent repeats of subunits. Biochemistry 45:13670–13676
32. Eftink MR (1991) Fluorescence quenching reactions: probing biological macromolecular structure. In: Dewey TG (ed) Biophysical and biochemical aspects of fluorescence spectroscopy. Plenum Press, New York, pp 1–41
33. Bradford MM (1976) A rapid and sensitive method for the quantitation of microgram quantities of protein utilizing the principle of protein-dye binding. Anal Biochem 72:248–254

34. Lakowicz JR (2006) Principles of fluorescence spectroscopy, 3rd edn. Springer, New York
35. Lehrer SS (1971) Solute perturbation of protein fluorescence. The quenching of the tryptophyl fluorescence of model compounds and of lysozyme by iodide ion. Biochemistry 10:3254–3263
36. Haldar S, Raghuraman H, Chattopadhyay A (2008) Monitoring orientation and dynamics of membrane-bound melittin utilizing dansyl fluorescence. J Phys Chem B 112:14075–14082
37. Eftink MR (1991) Fluorescence techniques for studying protein structure. Methods Biochem Anal 35:127–205
38. Burns NR, Ohanian V, Gratzer WB (1983) Properties of brain spectrin (fodrin). FEBS Lett 153:165–168
39. Mukherjee S, Chattopadhyay A (1995) Wavelength-selective fluorescence as a novel tool to study organization and dynamics in complex biological systems. J Fluoresc 5:237–246
40. Chattopadhyay A (2003) Exploring membrane organization and dynamics by the wavelength-selective fluorescence approach. Chem Phys Lipids 122:3–17
41. Raghuraman H, Kelkar DA, Chattopadhyay A (2005) Novel insights into protein structure and dynamics utilizing the red edge excitation shift approach. In: Geddes CD, Lakowicz JR (eds) Reviews in Fluorescence 2005, vol 2. Springer, New York, pp 199–222
42. Demchenko AP (2008) Site-selective red-edge effects. Methods Enzymol 450:59–78
43. Haldar S, Chaudhuri A, Chattopadhyay A (2011) Organization and dynamics of membrane probes and proteins utilizing the red edge excitation shift. J Phys Chem B 115:5693–5706
44. Chattopadhyay A, Haldar S (2014) Dynamic insight into protein structure utilizing red edge excitation shift. Acc Chem Res 47:12–19
45. Rawat SS, Kelkar DA, Chattopadhyay A (2004) Monitoring gramicidin conformations in membranes: a fluorescence approach. Biophys J 87:831–843
46. Raghuraman H, Chattopadhyay A (2003) Organization and dynamics of melittin in environments of graded hydration: a fluorescence approach. Langmuir 19:10332–10341
47. Rawat SS, Mukherjee S, Chattopadhyay A (1997) Micellar organization and dynamics: a wavelength-selective fluorescence approach. J Phys Chem B 101:1922–1929
48. Rawat SS, Chattopadhyay A (1999) Structural transition in the micellar assembly: a fluorescence study. J Fluoresc 9:233–244
49. Raghuraman H, Pradhan SK, Chattopadhyay A (2004) Effect of urea on the organization and dynamics of triton X-100 micelles: a fluorescence approach. J Phys Chem B 108:2489–2496
50. Kelkar DA, Chattopadhyay A (2004) Depth-dependent solvent relaxation in reverse micelles: a fluorescence approach. J Phys Chem B 108:12151–12158
51. Ghosh AK, Rukmini R, Chattopadhyay A (1997) Modulation of tryptophan environment in membrane-bound melittin by negatively charged phospholipids: implications in membrane organization and function. Biochemistry 36:14291–14305
52. Jain N, Bhasne K, Hemaswasthi M, Mukhopadhyay S (2013) Structural and dynamical insights into the membrane-bound α-synuclein. PLoS One 8:e83752
53. Guha S, Rawat SS, Chattopadhyay A, Bhattacharyya B (1996) Tubulin conformation and dynamics: a red edge excitation shift study. Biochemistry 35:13426–13433
54. Raja SM, Rawat SS, Chattopadhyay A, Lala AK (1999) Localization and environment of tryptophans in soluble and membrane-bound states of a pore-forming toxin from *Staphylococcus aureus*. Biophys J 76:1469–1479
55. Chaudhuri A, Haldar S, Chattopadhyay A (2010) Organization and dynamics of tryptophans in the molten globule state of bovine α-lactalbumin utilizing wavelength-selective fluorescence approach: comparisons with native and denatured states. Biochem Biophys Res Commun 394:1082–1086
56. Kelkar DA, Chaudhuri A, Haldar S, Chattopadhyay A (2010) Exploring tryptophan dynamics in acid-induced molten globule state of bovine α-lactalbumin: a wavelength-selective fluorescence approach. Eur Biophys J 39:1453–1463
57. Diakowski W, Prychidny A, Swistak M, Nietubyć M, Białkowska K, Szopa J, Sikorski AF (1999) Brain spectrin (fodrin) interacts with phospholipids as revealed by intrinsic fluorescence quenching and monolayer experiments. Biochem J 338:83–90
58. Demchenko A (1988) Red-edge-excitation fluorescence spectroscopy of single-tryptophan proteins. Eur Biophys J 16:121–129
59. Weber G, Shinitzky M (1970) Failure of energy transfer between identical aromatic molecules on excitation at the long wave edge of the absorption spectrum. Proc Natl Acad Sci U S A 65:823–830
60. Moens PDJ, Helms MK, Jameson DM (2004) Detection of tryptophan to tryptophan energy transfer in proteins. Protein J 23:79–83
61. Eftink MR (1991) Fluorescence quenching: theory and applications. In: Lakowicz JR (ed) Topics in fluorescence spectroscopy, vol 2. Plenum Press, New York, pp 53–126
62. Balter A, Nowak W, Pawelkiewicz W, Kowalczyk A (1988) Some remarks on the interpretation of the spectral properties of prodan. Chem Phys Lett 143:565–570
63. Samanta A, Fessenden RW (2000) Excited state dipole moment of PRODAN as determined from transient dielectric loss measurements. J Phys Chem A 104:8972–8975
64. Klein-Seetharaman J, Oikawa M, Grimshaw SB, Wirmer J, Duchardt E, Ueda T, Imoto T, Smith LJ, Dobson CM, Schwalbe H (2002) Long-range interactions within a nonnative protein. Science 295: 1719–1722
65. An X, Guo X, Zhang X, Baines AJ, Debnath G, Moyo D, Salomao M, Bhasin N, Johnson C, Discher D, Gratzer WB, Mohandas N (2006) Conformational stabilities of the structural repeats of erythroid spectrin and their functional implications. J Biol Chem 281:10527–10532
66. Baines AJ, Keating L, Phillips GW, Scott C (2001) The postsynaptic spectrin/4.1 membrane protein "accumulation machine". Cell Mol Biol Lett 6:691–702
67. Pielage J, Fetter RD, Davis GW (2006) A postsynaptic spectrin scaffold defines active zone size, spacing, and efficacy at the *Drosophila* neuromuscular junction. J Cell Biol 175:491–503
68. Patra M, Mukhopadhyay C, Chakrabarti A (2015) Probing conformational stability and dynamics of erythroid and nonerythroid spectrin: effects of urea and guanidine hydrochloride. PLoS One 10:e0116991
69. Shortle D (1993) Denatured states of proteins and their roles in folding and stability. Curr Opin Struct Biol 3:66–74
70. Schwalbe H, Fiebig KM, Buck M, Jones JA, Grimshaw SB, Spencer A, Glaser SJ, Smith LJ, Dobson CM (1997) Structural and dynamical properties of a denatured protein. Heteronuclear 3D NMR experiments and theoretical simulations of lysozyme in 8 M urea. Biochemistry 36:8977–8991
71. Shortle D, Ackerman MS (2001) Persistence of native-like topology in a denatured protein in 8 M urea. Science 293:487–489
72. McCarney ER, Kohn JE, Plaxco KW (2005) Is there or isn't there? The case for (and against) residual structure in chemically denatured proteins. Crit Rev Biochem Mol Biol 40:181–189
73. Kräutler V, Hiller S, Hünenberger PH (2010) Residual structure in a peptide fragment of the outer membrane protein X under denaturing conditions: a molecular dynamics study. Eur Biophys J 39:1421–1432
74. Chiarella S, Federici L, Di Matteo A, Brunori M, Gianni S (2013) The folding pathway of a functionally competent C-terminal domain of nucleophosmin: protein stability and denatured state residual structure. Biochem Biophys Res Commun 435:64–68